11th Australasian Fluid Mechanics Conference
University of Tasmania, Hobart, Australia
14-18 December 1992

BAROCLINIC VORTEX SIMULATION

F. LALLI[1], R. VERZICCO[2] and E. CAMPANA[1]

[1]INSEAN, Via di Vallerano139, 00128 Roma, ITALY

[2]Universita di Roma "La Sapienza", Via Eudossiana 18, 00185 Roma, ITALY

ABSTRACT

In the present paper a numerical study of the azimuthal instabilities of a baroclinic vortex, produced in a rotating tank, has been performed. The analisys has been carried out by direct simulation of 3-D Navier-Stokes equation, written in a rotating frame, by means of finite difference. The comparison with the available experimental data is satisfactory.

INTRODUCTION

In the dynamics of atmosphere and oceans, vortices play a fundamental role. For this reason the problem of vortices and their instabilities in rotating fluids, have been extensively studied in the last years (Saunders,1973 - Killworth,1980). Unstable meanders of the Gulf Stream, for example, are known to inject parcels of warm water in a colder environment in the north side and viceversa in the south side (Robinson,1983). Such isolated parcels generate baroclinic vortices whose evolution is regulated by the equilibrium among buoyancy, Coriolis and centrifugal forces. This flow structures are important for their property of heat and mass transport (salt, pollutants).

A simple way of producing a baroclinic vortex in laboratory (Griffiths and Linden,1981) is to allow a region of light fluid, initially constrained by a vertical cylinder, to adjust under gravity in a rotating tank: the light fluid parcel changes its shape, reaches the equilibrium configuration and then performs an oscillatory motion around it. The Coriolis force induces an anticyclonic vortex in the light fluid, and a cyclonic one in the deeper layer. In a subsequent phase non axisymmetric disturbances grow and modify the original circular shape of the front. The lighter fluid spreads radially generating smaller eddies , whose number depends on the Richardson parameter Ri and on the ratio $\delta = h/H$, where h is the initial depth of the light fluid layer, and H is the depth of the whole fluid domain (see fig. 1). Although a simplified model predicts a stability limit, neither in the experiments of Griffiths and Linden(1981), nor in our numerical simulations stable flows have been observed.

THE NUMERICAL METHOD

In a cylindrical rotating frame the equations of mass and momentum conservation are the following:

$$\nabla \cdot \mathbf{v} = 0 \tag{1}$$

$$\frac{d}{dt}\mathbf{v} = -\nabla p - \Delta\rho\left(\frac{\mathbf{k}}{D \cdot Ar} - \frac{1}{4Ri}\mathbf{r}\right) + \tag{2}$$
$$-\frac{1}{Ro}\mathbf{k} \times \mathbf{v} + \frac{1}{Re}\nabla^2\mathbf{v}$$

The equation for the density can be written as follows:

$$\frac{d}{dt}\Delta\rho = \frac{1}{Re \cdot Sm}\nabla^2\Delta\rho \tag{3}$$

In (2) we have used the Boussinesq approximation for density variation.

The equations have been non-dimensionalized with respect to the characteristic length, velocity and time, chosen respectively as a (radius of cylindrical zone of light fluid), $U = \sqrt{hg\prime}$ and $T = \sqrt{\frac{a^2}{hg\prime}}$; $g' = g\frac{\Delta\rho_0}{\rho_0}$ is the reduced gravity. The following parameters are so obtained:

$$D = \frac{\Delta\rho_0}{\rho_0}; \quad Ar = \frac{h}{a}; \quad Ri = \frac{hg\prime}{4\Omega^2 a^2}$$

$$Ro = \frac{U}{2\Omega a}(= \sqrt{Ri}); \quad Re = \frac{Ua\rho_0}{\mu}; \quad Sm = \frac{\mu}{\rho_0 \epsilon}$$

where ϵ is the diffusivity of the salt in water.

Navier-Stokes equations have been solved with free-slip conditions at the external boundaries (only at the tank bottom no-slip conditions have been implemented), while for the density equation the following boundary condition has been satisfied:

$$\frac{\partial}{\partial n}\Delta\rho = 0.$$

The numerical scheme used is described in details in the paper by Verzicco and Orlandi(1992), here

we summarize only the main features. The system of equations have been solved by a fractional step method (Kim and Moin,1985). Both viscous and advective terms have been discretized by centered 2nd order finite difference schemes; the viscous ones have been calculated implicitly, while the advective ones explicitly. In the 3–D case, in the limit of $\mu \rightarrow 0$, the energy should be conserved: such property holds for the discrete scheme used.

At each time step a non-solenoidal field velocity is calculated by using the pressure at the old time step; a scalar quantity Φ is then introduced to project the non-solenoidal field in a solenoidal one.

The advancement in time of the solution has been obtained by a hybrid 3-step Runge-Kutta method.

RESULTS

This phenomenon of instability has been studied in the present paper starting from the experimental results obtained by Griffiths and Linden(1981). The flow is initially driven by the buoyancy forces; conservation of angular momentum implies the formation of an anticyclonic flow in the upper layer and a cyclonic circulation in the lower layer. Such structures have been observed experimentally and they are clearly reproduced by the numerical simulations (fig.2). In fig.3 the case without tank rotation is depicted: the flow is characterized only by the baroclinic vorticity production; buoyancy forces are not balanced by Coriolis and centrifugal forces: in this case the adjustment is very fast, and the free surface between the fluids overturns, performing a breaking wave.

When the initial circular shape of the light fluid is perturbed, the flow is no longer axisymmetric. The numerical results show the onset and growth of instabilities at the front, with generation of eddies.

Fig 4,5 show the cases of perturbation wavenumber n=2,3, in a qualitative comparison with the experimental results obtained by Griffiths and Linden. In this case the simulation starts from a configuration with a sinusoidal perturbation.

In order to recognize what is the 'natural' unstable wavenumber a lot of cases with initial random perturbation have been simulated; in fig.6 one of these cases is shown, in particular when four eddies are generated. By using the spectral analisys of the velocity field the growth rate of the unstable wavenumber in the different situations has been analised. As in the experimental results, there are some flows in which several wavenumbers seem to be unstable; anyway, fig. 7 shows that our results are in a rather good agreement with the experimental results.

AKNOWLEDGEMENTS

The authors are indebted to Professor Paolo Orlandi (University of Roma), for valuable discussions and suggestions and for the graphic facilities. The work was supported by the Italian Ministry of Merchant Marine in the frame of INSEAN research plan 1988-90.

REFERENCES

GRIFFITHS R.W., LINDEN P.F. (1981) The Stability of Vortices in a Rotating, Stratified Fluid, J. Fluid Mech., **105**.

KILLWORTH P.D. (1980) Barotropic and Baroclinic Instability in Rotating Stratified Fluids, Dyn. of Atmos. and Oceans, **4**.

KIM J., MOIN P. (1985) Application of a Fractional Step Method to Incompressible Navier-Stokes Equations, J. Comp. Phys., **59**.

ROBINSON A.R. (1983) Eddies in Marine Science, Springer & Verlag Berlin 609 pp.

SAUNDERS P.M. (1973) The Instability of Baroclinic Vortex, J. Physical Ocean., **3**.

VERZICCO R., ORLANDI P. (1992) A Finite Difference Scheme for Direct Simulation in Cylindrical Coordinates, Proc. ICOSAHOM, Int. Conf. on Spectral and Higher Order Methods, Montpellier, France.

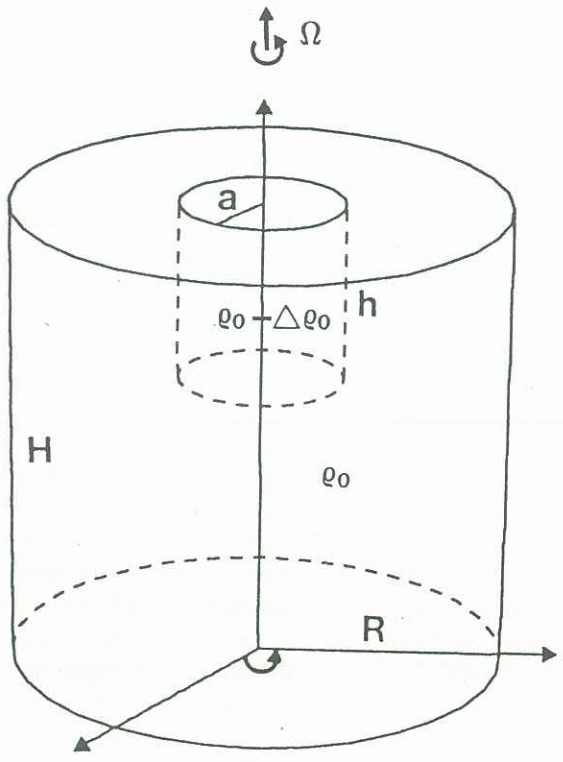

Fig.1 The numerical rotating tank.

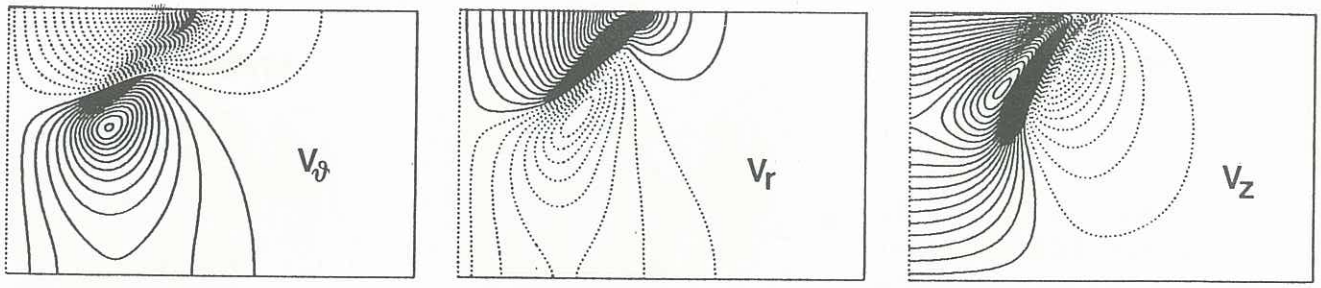

Fig.2 Axisymmetric flow ($Ar = 1.$, $\delta = .5$, $D = 10^{-3}$, $Sm = 1.$, $Ri = 0.2628$, $Re = 1025.357$): generation of cyclonic and anticyclonic circulations; contour lines for positive(solid) and negative values(dashed) of velocity.

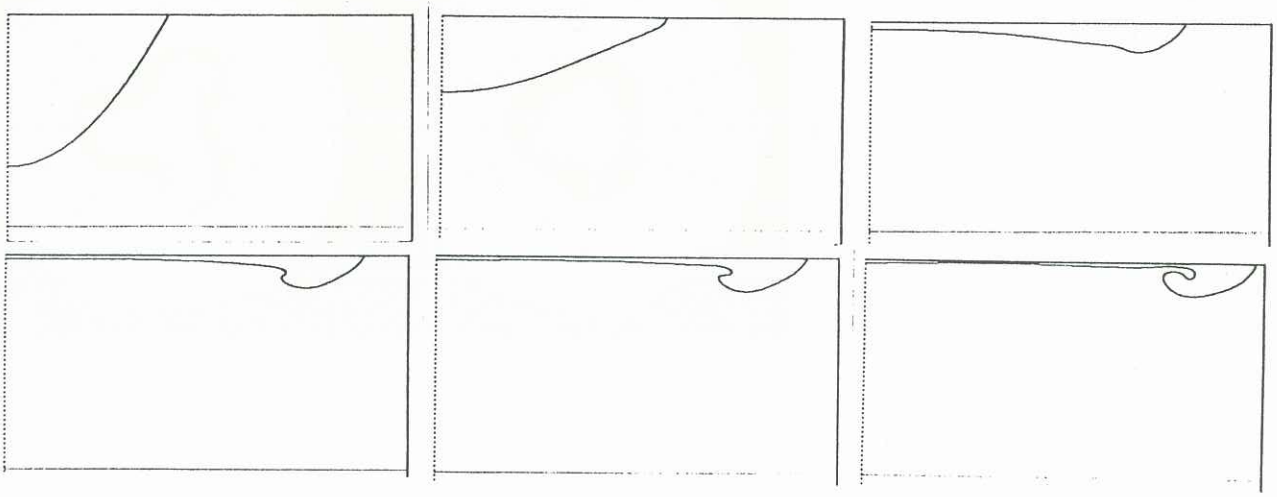

Fig.3 Axisymmetric flow without tank rotation ($Ar = 1.$, $\delta = .5$, $D = .02$, $Sm = 1.$, $Ri = \infty$, $Re = 4585.534$): evolution of the interface between the two fluids.

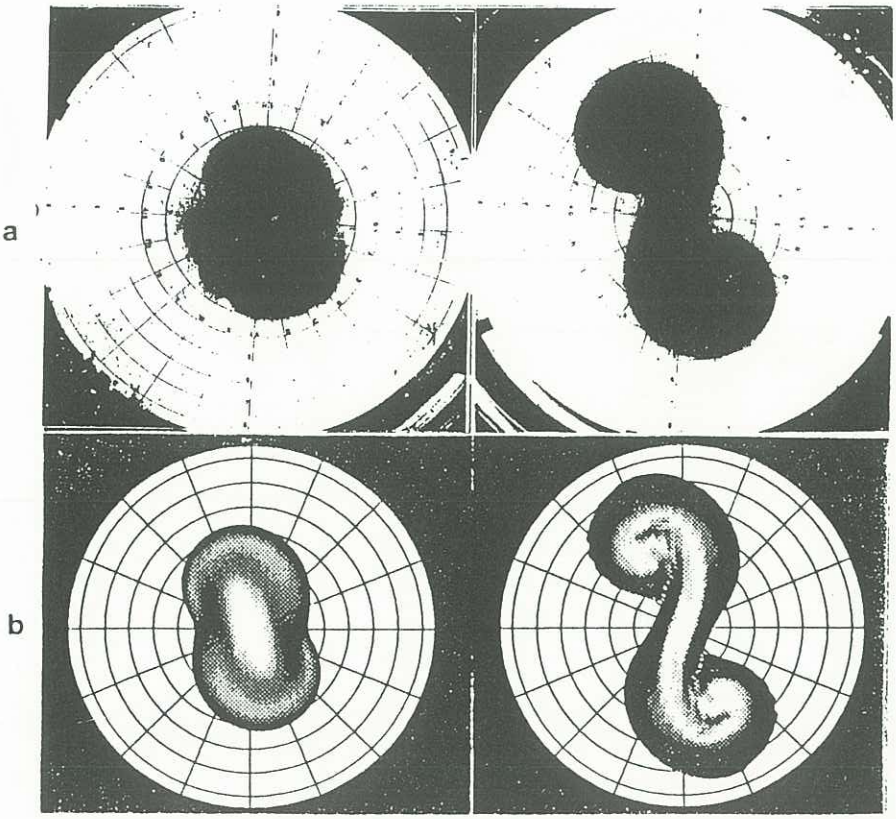

Fig.4 Fully 3-D flow: evolution of sinusoidal initial perturbation (azimuthal wavenumber n=2, $Ar = 1.$, $\delta = .5$, $D = 10^{-3}$, $Sm = 1.$, $Ri = .2628$, $Re = 1025.357$):
a) Experimental plan view photographs
b) Numerical isopycnal surfaces.

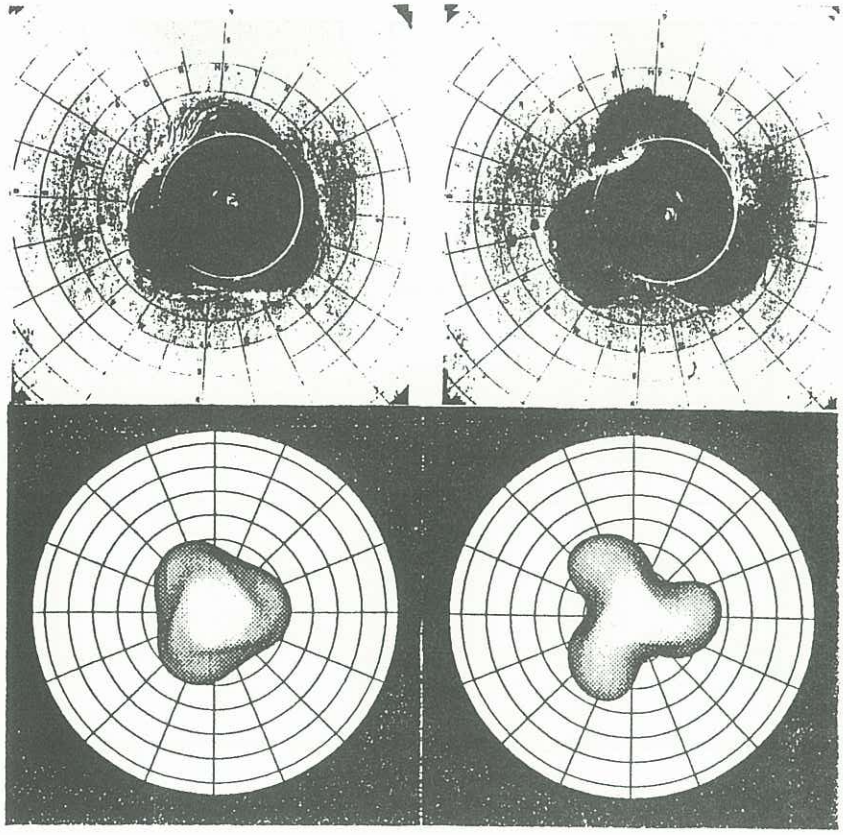

Fig.5 Fully 3–D flow: evolution of sinusoidal initial perturbation (azimuthal wavenumber n=3, $Ar = 1.$, $\delta = .5$, $D = 5.7 * 10^{-4}$, $Sm = 1.$, $Ri = .1498$, $Re = 774.127$):
a) Experimental plan view photographs
b) Numerical isopycnal surfaces.

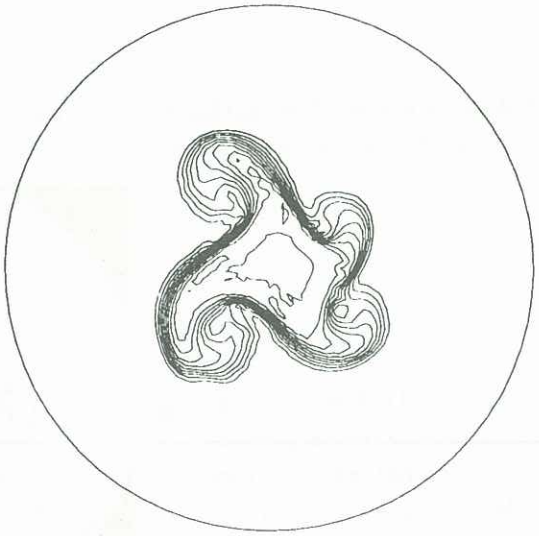

Fig.6 Fully 3–D flow: evolution of a random initial perturbation. $Ar = 1.2857$, $\delta = .6$, $D = 7 * 10^{-4}$, $Sm = 1.$, $Ri = .09$, $Re = 1740.21$).

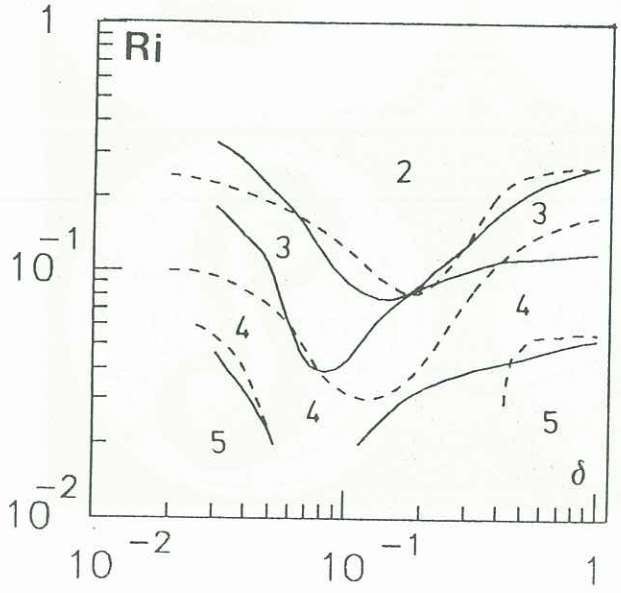

Fig.7 Fully 3 D flow: evolution of random initial perturbations. Azimuthal wavenumber as a function of $Ri = hg'/4\Omega^2 a^2$ and $\delta = h/H$. The lines, drawn 'by eye', divide the plane (Ri, δ) into regions in which different wavenumbers seem to be more unstable.
a) Solid lines: experiments by Griffiths and Linden(1981)
b) Dashed lines: numerical simulations.